

Quasiparticle thermal Hall angle and magnetoconductance in $\text{YBa}_2\text{Cu}_3\text{O}_x$.

K. Krishana, N. P. Ong, Y. Zhang, and Z. A. Xu[†]

Joseph Henry Laboratories of Physics, Princeton University, Princeton, New Jersey 08544

R. Gagnon and L. Taillefer[§]

Department of Physics, McGill University, Montreal, Quebec, Canada

(August 8, 2018)

We present a way to extract the quasiparticle (*qp*) thermal conductivity κ_e and mean-free-path in $\text{YBa}_2\text{Cu}_3\text{O}_x$, using the thermal Hall effect and the magnetoconductance of κ_e . The results compare well with heat capacity experiments. Moreover, we find a simple relation between the thermal Hall angle θ_Q and the H -dependence of κ_e , as well as numerical *equality* between θ_Q and the electrical Hall angle. The results also reveal an anomalously anisotropic scattering process in the normal state.

74.25.Fy, 74.72.Bk, 72.15.Gd, 74.60.Ge

The quasiparticle excitations in cuprate superconductors display many unusual properties related to their long transport lifetimes and the existence of nodes in the gap function. These properties have been investigated by microwave and heat transport techniques. Bonn *et al.* [1] uncovered a broad peak in the zero-field microwave conductivity in $\text{YBa}_2\text{Cu}_3\text{O}_7$ (YBCO). From measurements of the the zero-field thermal conductivity anomaly in untwinned YBCO, Yu *et al.* [2] inferred that it arises entirely from the quasiparticles. Taillefer *et al.* [3] measured values of κ_{xx} below 0.1 K that are close to the predicted universal value κ_e^{00} [4].

The long quasiparticle lifetime also produces a large thermal Hall effect which has been investigated in YBCO [5]. While the quasiparticles are solely responsible for the thermal Hall conductivity κ_{xy} , their contribution to the diagonal conductivity κ_{xx} is harder to sort out experimentally. The general problem of *qp* transport in a d -wave superconductor in a field is an active area of research [6–9]. Novel effects such as those arising from the doppler-shift term [7], field quantization of the states around the nodes [8], and Andreev scattering from a disordered vortex array [9] have been proposed.

We report results that reveal a close relation between κ_{xy} and κ_{xx} in YBCO. We find that the thermal Hall angle θ_Q closely tracks a parameter $p(T)$ extracted from the field dependence of κ_{xx} , which implies strongly that $p(T)$ is proportional to the *qp* mean-free-path (mfp). In addition, we find that θ_Q agrees *numerically* with the electrical Hall angle θ_e extrapolated from above T_c . Our results disagree with the factor of 2 discrepancy found in a recent related study [10].

Measurements of κ_{xx} and κ_{xy} were made on 4 crystals (1-4) in a field $\mathbf{H} \parallel \mathbf{c}$. Samples 1 and 2 are both optimally doped and detwinned with $x = 6.95$ and $T_c = 93.3$ K. With the thermal current $\mathbf{J}_Q \parallel \hat{\mathbf{x}} \parallel \mathbf{a}$, the thermal gradient $-\partial_x T$ is measured with a pair of matched cernox sensors. The antisymmetric ‘Hall’ gradient $-\partial_y T \parallel \mathbf{b}$ (the chain axis) is measured with a pair of chromel-constantan thermocouples, as in [5]. Samples 3 and 4 are underdoped

twinned crystals with $T_c = 63$ and 60 K, respectively (in both $x = 6.63$).

As our analysis rests on the finding that κ_{ph} (the phonon conductivity) is insensitive to H , we first summarize the evidence for this result. In the cuprates, the field dependence of κ_{xx} is known to be described by the equation

$$\kappa_{xx}(H, T) = \frac{\kappa_e^0(T)}{(1 + p(T)|H|^\mu)} + \kappa_B(T), \quad (1)$$

where $p(T)$ is an inverse field scale and $\mu = 1$.

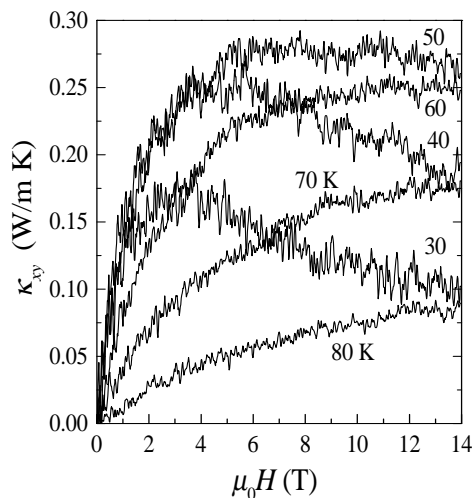


FIG. 1. The Hall conductivity κ_{xy} in untwinned $\text{YBa}_2\text{Cu}_3\text{O}_7$ (sample 1), with thermal current $\mathbf{J}_Q \parallel \mathbf{a}$ and $\mathbf{H} \parallel \mathbf{c}$.

Equation 1 has been tested at high resolution. In underdoped YBCO (in which $p(T)$ approaches 4 T^{-1} and a plateau value is observed below 15 K), κ_{xx} fits Eq. 1 closely over 2 decades in H [11]. These fits require the background term κ_B to be H -independent [5,12] (see also Yu *et al.* [13]). Thus, these earlier findings impose the constraint that either the *qp* conductivity or the phonon conductivity must be H -independent.

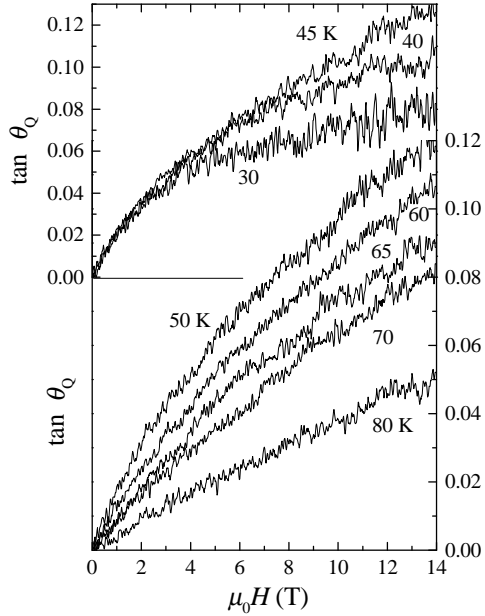


FIG. 2. Traces of the Hall angle $\tan \theta_Q = \kappa_{xy}/\kappa_e$ where $\kappa_e \equiv \kappa_{xy} - \kappa_B$, with κ_B determined by fitting to Eq. 1 (sample 1).

Because κ_{xy} displays strong curvature vs. H , the phonon term is clearly the one that is H -independent. Hence, in Eq. 1, we identify the difference $\kappa_{xx} - \kappa_B$ with the field-dependent part of the a -axis qp conductivity $\kappa_{e,a}(H, T)$ (we have written $\kappa_e^0 = \kappa_{e,a}(0, T)$). The H -independent term κ_B is identified with κ_{ph} , including possibly a very small residual electronic term κ_e^{00} that is H -independent [9]. With $\kappa_{e,a}$ so extracted, we may obtain the thermal Hall angle $\tan \theta_Q \equiv \kappa_{xy}(H, T)/\kappa_{e,a}(H, T)$ (hereafter we drop the a in $\kappa_{e,a}$).

The Hall conductivity κ_{xy} in sample 1 (see Fig. 1) displays behavior similar to that in Ref. [5], but with stronger curvature vs. H . Results for samples 2 are closely similar. Combining κ_{xy} and the parameters in Eq. 1, we derive $\tan \theta_Q$. The traces in Fig. 2 show that $\tan \theta_Q$ is initially linear in H , but displays increasing curvature at large H and low T . We focus only on the initial value.

The weak-field $\tan \theta_Q$ provides a powerful clue to the meaning of $p(T)$. Comparing the two quantities (main panel of Fig. 3), we note that $p(T)$ increases rapidly with decreasing T , closely tracking θ_Q . Between 30 and 80 K, the data for $p(T)$ and θ_Q (open triangles) may be made to lie on the same curve, if we simply divide $p(T)$ by the dimensionless scale factor $\mathcal{M} \equiv p(T)B/\theta_Q$ ($B \rightarrow 0$) (in both 1 and 2, \mathcal{M} equals 13). Thus, the two quantities share the same T dependence over a broad range of T .

As $\tan \theta_Q$ is generally proportional to the qp lifetime, the comparison implies that $p(T)$ is also proportional to the qp lifetime or mean-free-path $\ell(T)$. It is then convenient to express $p(T)$ in the general form

$$p(T) = \ell(T)s/\phi_0, \quad (2)$$

where the length scale s depends on the particular model,

and $\phi_0 = h/2e$ (h is Planck's constant and e is the elementary charge).

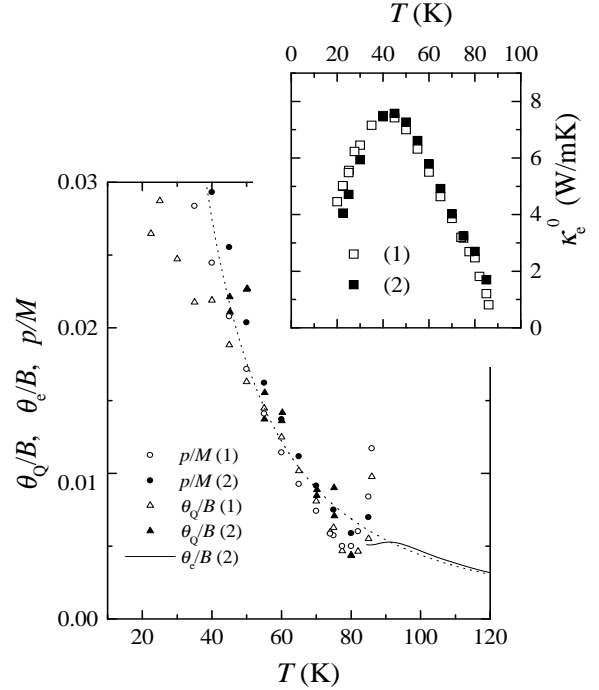


FIG. 3. [Main panel] Comparison of the parameter $p(T)/M$ in samples 1 (open circles) and 2 (solid circles), with the weak-field θ_{QP}/B in 1 (open triangles) and 2 (solid triangles). The solid lines are values of θ_e/B measured in sample 2 above 93 K (the broken line shows its extrapolation as the curve $44/T^2$). The inset shows the zero-field qp conductivity κ_e^0 extracted in 1 and 2.

We may also express the initial Hall-angle in terms of a ‘Hall-angle’ mean-free-path ℓ_H , viz. $\theta_Q = \ell_H(T)eB/\hbar k_F$ with k_F the Fermi wavevector. Proportionality between $p(T)$ and $\tan \theta_Q$ implies

$$s = (\ell_H/\ell)(\mathcal{M}\pi/k_F) \simeq 65(\ell_H/\ell) \text{ \AA}, \quad (3)$$

with $k_F \simeq 0.64 \text{ \AA}^{-1}$.

We add the caveat that, in 93-K YBCO, the simple proportionality between $p(T)$ and ℓ expressed in Eq. 2 does not hold close to T_c . Above 80 K, the extracted $p(T)$ and θ_Q appear to diverge as $T \rightarrow T_c^-$. This divergence is an artifact produced by the existence of a sharp zero-field cusp in the $\kappa_{xx} - H$ profile close to T_c (its presence enhances the slope of κ_{xx} vs. H as $H \rightarrow 0$). In 93-K YBCO, the cusp smoothly merges into the regular profile and cannot be isolated easily. Thus, the apparent $p(T)$ is increasingly distorted as we get close to T_c . However, in underdoped YBCO, the cusp is clearly distinct from the regular profile and its effect may be subtracted (see inset in Fig. 4). The origin of the cusp is unknown at present.

Recent heat capacity experiments on YBCO place strong constraints on the analysis of κ_e^0 at low T , which we now address. The qp thermal conductivity $\kappa_e^0(H=0)$

extracted for samples 1 and 2 are displayed in the inset in Fig. 3. As T decreases, κ_e^0 increases by ~ 10 before decreasing rapidly. We may write $\kappa_e^0 = c_e \langle v\ell \rangle / 2$ where c_e is the electronic heat capacity and $\langle v\ell \rangle$ denotes the group velocity- mfp product averaged over the Fermi Surface. The weak-field Hall conductivity is $(c_e \langle v\ell \rangle / 2) \tan \theta_Q$. At low T in a d -wave superconductor, the Boltzmann-equation approach gives $\langle v\ell \rangle = (v_1 \ell_1 + v_2 \ell_2) / 2$, where subscripts 1 and 2 refer to the principal axes of the Dirac cone at the nodes (as $v_1/v_2 \simeq 7$, transport along the 1-axis dominates). Dividing the two conductivities by ℓ_1 and ℓ_1^2 , respectively, gives quantities that may be compared with c_e . Although $p(T)$ in our experiment determines ℓ_1 only up to the unknown parameter s , we may plot our data as $\kappa_e^0/p(T)$ and $\kappa_{xy}(0)/Bp(T)^2$, and examine their T dependence (Fig. 4). Below 60 K, both are consistent with a power-law T dependence (in particular, $\kappa_{xy}(0)/Bp(T)^2$ fits a T^2 behavior).

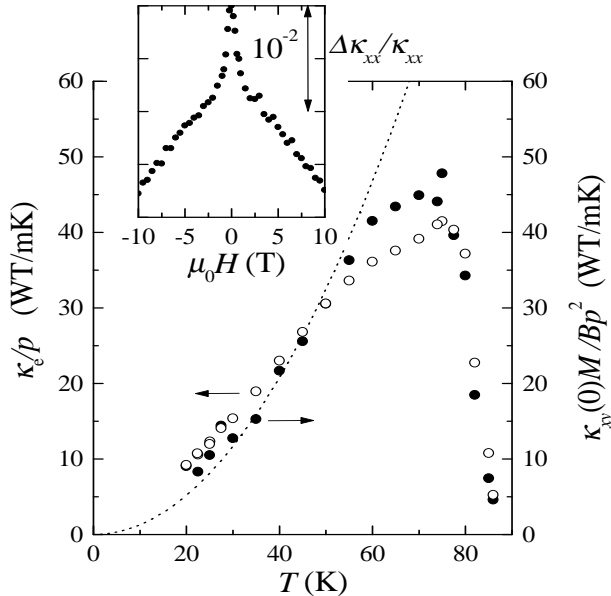


FIG. 4. (Main panel) The T dependence of $\kappa_e/p(T)$ (open circles) and $\kappa_{xy}(0)/Bp(T)^2$ (solid circles) in sample 1. Both quantities are proportional to c_e ($\kappa_{xy}(0)$ is multiplied by \mathcal{M}). From the value of α reported by Wright *et al.*, we have calculated κ_e^0/ℓ_1 , and plotted it as $(\kappa_e^0/\ell_1) \times (\phi_0/s)$ with $s = 45 \text{ \AA}$ (the broken line = $0.013 T^2 \text{ TW/Km}$). The inset shows the cusp anomaly in κ_{xx} vs. H at 55 K in underdoped YBCO.

The heat capacity measurements appear to be converging to the result that, at $H=0$, c_e varies as αT^2 at low T , with $\alpha \simeq 0.064 \text{ mJK}^{-3} \text{ mol}^{-1}$ [15]. This value of α implies [16] $v_1 = v_F = 1.78 \times 10^7 \text{ cm/s}$ and $\kappa_e^0/\ell_1 = 2.72 \times 10^4 T^2$. By comparing the second equation with our results, we can fix the unknown scale s . The best fit (broken line in Fig. 4) gives $s = 45 \text{ \AA}$, in reasonable agreement with Eq. 3. With this s in Fig. 3, we find that $\ell_1 \simeq 1,800 \text{ \AA}$ at 40 K.

We next compare the T dependence of $\tan \theta_Q$ with the electrical Hall angle $\tan \theta_e = \rho_{xy}/\rho_b$ (the solid line in

Fig. 3, main panel). Remarkably, $\tan \theta_Q$ falls on the $1/T^2$ curve of $\tan \theta_e$ extrapolated to below 93 K with no adjustments to either scale (dotted line). In YBCO, a large fraction ($\sim 1/2$) of the charge carriers are in the chains ($\parallel \mathbf{b}$). Because of the resistivity anisotropy $\rho_a/\rho_b (=2.1$ at 100 K), it is important that we compare $\tan \theta_Q$ with the correct Hall angle ρ_{xy}/ρ_b (this probes the electrical current $\parallel \mathbf{a}$; the incorrect choice ρ_{xy}/ρ_a is only half as large). Hence, our finding of numerical agreement between $\tan \theta_Q$ and $\tan \theta_e$ applies strictly to the carriers in the CuO_2 plane. The case for $\mathbf{J}_Q \parallel \mathbf{b}$ remains to be investigated. Nevertheless, when twinned crystals are used (see 3 and 4), we still observe *equality* between the two Hall angles. This suggests that the equality holds as well when $\mathbf{J}_Q \parallel \mathbf{b}$. Thus, our overall finding is inconsistent with that of Zeini *et al.* who find that $\theta_Q/\theta_e \simeq 2$ in a twinned crystal [10].

The results in the underdoped 60-K crystals provide important complementary information. We may extend measurements of $p(T)$ to lower T (10 K) because flux pinning is much weaker. Further, the cusp near T_c is readily separated from the regular H dependence of κ_{xx} (inset of Fig. 4), so $p(T)$ may be reliably determined up to T_c . In the main panel of Fig. 5, we display $p(T)$ measured in samples 3 and 4 (open triangles and circles, respectively). With increasing T , $p(T)$ falls rapidly. The T dependence of θ_Q (solid symbols) is closely similar. By adjusting \mathcal{M} ($= 20$ and 15 for samples 3 and 4, respectively), we may also match the curves for θ_Q and $p(T)$. We emphasize that $p(T)$ does not show a divergence near T_c , unlike the case in 1 and 2. Moreover, as T increases above 55 K, $p(T)/\mathcal{M}$ falls *below* the curve for θ_e/B . Also shown are data for the electrical Hall angle θ_e measured in 4 (crosses).

In the inset in Fig. 5, we display the same data over a broader range of T (10 to 240 K). The log-log plot shows that θ_Q continues on the curve for θ_e extrapolated below T_c (without any scale adjustment). Between T_c and 100 K, the upper curve displays an apparent broad minimum. This shallow feature is the superposition of a rapidly decreasing $\tan \theta_e$ (as $T \rightarrow T_c^+$) and a rapidly increasing $\tan \theta_Q$ as T decreases below T_c . A recent investigation reveals that the decrease in $\tan \theta_e$ is correlated with the opening of the pseudogap at 150 K [17]. This causes the Hall angle to plummet steeply relative to its high- T trend. The inset shows rather clearly that, apart from the dip, θ_Q is continuous with the normal-state θ_e .

It is instructive to re-express the underdoped results in terms of mean-free-paths. Over the interval 30-55 K, ℓ and ℓ_H are proportional. If we assume $\ell \simeq \ell_H$, we may use the scale factor \mathcal{M} to convert $p(T)$ and θ_Q into mfp 's. In the inset in Fig. 5 (right axis) we have expressed $p(T)$ and θ_Q in terms of ℓ . We find that ℓ decreases rapidly from 4,000 to 550 \AA between 10 and 50 K. Above T_c , however, ℓ and ℓ_H follow different curves. Whereas ℓ_H smoothly joins the $1/T^2$ Hall-angle curve in the normal state, ℓ derived from $p(T)$ sharply decreases

across T_c (open symbols), assuming values above 55 K much shorter than ℓ_H . The sharp reduction in ℓ is consistent with the transport mfp (diamonds) deduced from the in-plane resistivity ρ [18].

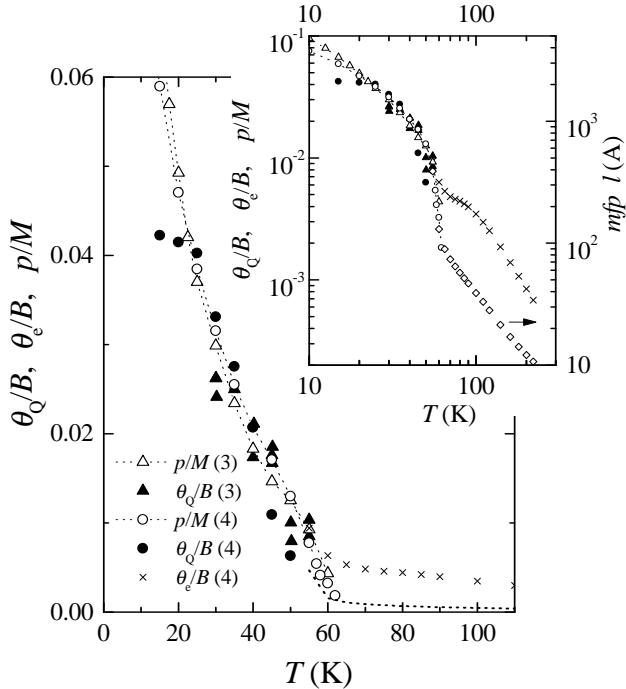


FIG. 5. [Main panel] The T dependence of $p(T)/M$ (open symbols) and θ_Q/B (solid symbols) in underdoped YBCO (samples 3 and 4). Data for θ_e/B above 60 K (from 4) are shown as an \times . The inset shows the same data in log-log scale to emphasize that θ_Q is continuous with θ_e except for a ‘dip’ between 60 and 100 K associated with the opening of the pseudogap. The right axis represents the data in terms of ℓ and ℓ_H (see text). The diamonds are values for ℓ obtained from the in-plane ρ measured in 4 (also shown as a dotted line in main panel).

It appears that, starting about 10 K below T_c , a novel scattering mechanism Γ_{tr} becomes prominent and grows rapidly with T . It selectively damps the longitudinal current, but does not seem to affect the transverse (Hall) current. Thus, ℓ decreases more rapidly than ℓ_H across T_c , resulting in the two branches shown in the inset of Fig. 5. The two branches recall the two-lifetime scenario in the Hall-angle experiment of Chien *et al.* [19].

In summary, we have combined measurements of κ_{xx} vs. H with κ_{xy} to achieve a self-consistent separation of the qp and phonon conductivities. The numerical agreement between the thermal and electrical Hall angles in both twinned and untwinned crystals, and the comparison with heat capacity experiments support the validity of the analysis presented.

We thank P. W. Anderson, M. Franz, and F.D.M. Haldane for many discussions. N.P.O. acknowledges support from the U.S. Office of Naval Research (N00014-90-J-1013) and the U.S. National Science Foundation

(DMR98-09483).

† Permanent address of ZAX: Department of Physics, Zhejiang University, Hangzhou, China.

§ Present address of LT: Department of Physics, University of Toronto, Toronto, Ontario, Canada M5S 1A7.

-
- [1] D. A. Bonn *et al.*, Phys. Rev. Lett. **68**, 2390 (1992); D. A. Bonn *et al.*, Phys. Rev. B **50**, 4051 (1994); W. N. Hardy *et al.* Phys. Rev. Lett. **70**, 3999 (1993).
 - [2] R. C. Yu *et al.*, Phys. Rev. Lett. **69**, 1431 (1992).
 - [3] L. Taillefer *et al.*, Phys. Rev. Lett. **79**, 483 (1997).
 - [4] M. Graf *et al.*, Phys. Rev. B **53**, 15147 (1996).
 - [5] K. Krishana, J. M. Harris, and N. P. Ong, Phys. Rev. Lett. **75**, 3529 (1995).
 - [6] Steve H. Simon and Patrick A. Lee, Phys. Rev. Lett. **78**, 1548 (1997).
 - [7] C. Kubert and P. J. Hirschfeld, Phys. Rev. Lett. **80**, 4693 (1998).
 - [8] Philip W. Anderson, cond-mat/9812063.
 - [9] M. Franz, Phys. Rev. Lett. **82**, 1760 (1999).
 - [10] B. Zeini *et al.*, Phys. Rev. Lett. **82**, 2175 (1999). The factor of 2 discrepancy in Zeini’s work may arise from their starting assumption that $\tan\theta_Q$ is strictly H -linear (see our Fig. 2).
 - [11] K. Krishana, Y. Zhang, Z. A. Xu, and N. P. Ong, *to be published*; N.P. Ong *et al.* in *Physics and Chemistry of Transition Metal Oxides*, edited by H. Fukuyama and N. Nagaosa (Springer-Verlag, 1999), p. 202.
 - [12] K. Krishana *et al.*, Science **277**, 83 (1997).
 - [13] F. Yu *et al.*, Physica C **267**, 308 (1996).
 - [14] Xiao-Gang Wen and Patrick A. Lee, Phys. Rev. Lett. **80**, 2193 (1998); P. A. Lee and X. G. Wen, *ibid.* **78**, 4111 (1997).
 - [15] D. A. Wright *et al.*, Phys. Rev. Lett. **82**, 1550 (1999). The spread of values found for α is discussed by Wright *et al.*
 - [16] At low T , c_e is given by $4\eta k_B^3 T^2 / (\pi d \hbar^2 v_F v_2)$, where $d = 5.8 \text{ \AA}$, v_f and v_2 are the principal-axis velocities, and $\eta = \int_0^\infty dx x^3 (-\partial f / \partial x) \simeq 5.41$. With $v_F / v_2 = 7$, we find $v_F = 1.78 \times 10^7 \text{ cm/s}$.
 - [17] Z.A. Xu, Y. Zhang, and N. P. Ong, cond-mat/990312.
 - [18] From the measured ρ ($70 \mu\Omega\text{cm}$ at 70 K), we find $k_F \langle \ell \rangle = 22$, which gives a lower bound to the mfp of 34 \AA . We estimate that near the nodes ℓ is about 3 times larger.
 - [19] T. R. Chien *et al.* Phys. Rev. Lett. **67**, 2088 (1991); P. W. Anderson, Phys. Rev. Lett. **67**, 2092 (1991).